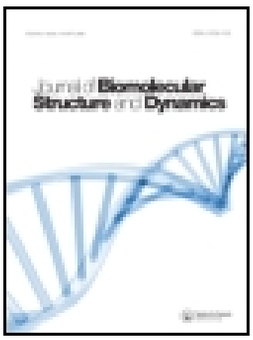

Taylor & Francis
Taylor & Francis Group

Journal of Biomolecular Structure and Dynamics

ISSN: 0739-1102 (Print) 1538-0254 (Online) Journal homepage: http://www.tandfonline.com/loi/tbsd20

Structural, functional and molecular dynamics analysis of the native and mutated actin to study its effect on congenital myopathy

Faeze Sadat Mohajer, Sepideh Parvizpour, Jafar Razmara, Mahsa Khoshkhooy Yazdi & Mohd Shahir Shamsir

To cite this article: Faeze Sadat Mohajer, Sepideh Parvizpour, Jafar Razmara, Mahsa Khoshkhooy Yazdi & Mohd Shahir Shamsir (2016): Structural, functional and molecular dynamics analysis of the native and mutated actin to study its effect on congenital myopathy, Journal of Biomolecular Structure and Dynamics, DOI: 10.1080/07391102.2016.1190299

To link to this article: http://dx.doi.org/10.1080/07391102.2016.1190299

Journal of Biomolecular Structure and Dynamics, 2016
http://dx.doi.org/10.1080/07391102.2016.1190299

LETTER TO THE EDITOR

Structural, functional and molecular dynamics analysis of the native and mutated actin to study its effect on congenital myopathy

Faeze Sadat Mohajer[a], Sepideh Parvizpour[b], Jafar Razmara[c], Mahsa Khoshkhooy Yazdi[d] and Mohd Shahir Shamsir[a]*

[a]*Bioinformatics Research Group, Faculty of Bioscience and Medical Engineering, UniversitiTeknologi Malaysia, Johor Bahru, Malaysia;* [b]*Biotechnology Research Center, Tabriz University of Medical Sciences, Tabriz, Iran;* [c]*Departement of Computer Science, University of Tabriz, Tabriz, Iran;* [d]*Faculty of Science, Department of Chemistry, Universiti Teknologi Malaysia, 81310 UTM, Johor, Malaysia*

Communicated by Ramaswamy H. Sarma

(*Received 9 January 2016; accepted 12 May 2016*)

Introduction

Congenital myopathies are a broad group of genetic muscular malfunctions which are detectable since birth. More than 170 mutations have been discovered in the gene of skeletal muscle α-actin (ACTA-1) to be responsible for five categories of overlapping congenital myopathies. These myopathies are known as nemaline myopathy, intranuclear rod myopathy, actin filament aggregate myopathy, congenital fiber-type disproportion, and myopathy with core-like area (Laing et al., 2009). Ser350Leu is one of the mutations that has been assigned for actin filament aggregate myopathy. This is a fatal disease in which actin-containing filaments are being accumulated in the muscle fibers and causes an early death due to severe respiratory problems (Goebel & Müller, 2006). In the wild type, Serine 350 is one of the amino acids that forms a hydrogen bond with myosin during a muscular contraction. The alcoholic group of this amino acid forms a hydrogen bond with the oxygen atom of Lysine 639 of S1 subdomain of myosin (Lorenz & Holmes, 2010). In an actomyosin cycle, myosin interacts with two adjacent actin monomers in an actin filament by hydrolyzing an adenosine triphosphate (ATP) molecule which is coupled with magnesium ion (Mg^{2+}). Any mutation that changes the structure of actin monomers affects the whole actin filament conformation.

Although S350L has been attributed to actin filament aggregate myopathy, the effects of this mutation on three-dimensional (3D) structure and function of actin has not been studied yet. In 2003, three cross-linked actin monomer (AC1, AC2, and AC3) of F-actin have been crystalized by Dawon et al. for the first time (Dawson, Sablin, Spudich, & Fletterick, 2003). It has been known that myosin mostly interacts with AC3 during a power stroke stage of actomyosin cycle. S350L has been detected to be in the location of myosin and AC3 interactions. The aim of this study is to investigate the effects of S350L on the structure of actin and the formation of hydrogen bond between myosin and actin. To achieve a proper analysis, both wild and mutated types of actin and myosin have been modeled and simulated using molecular dynamics simulation. Then, the simulated models of actin have been structurally analyzed in a comparative study. Eventually, myosin has been docked with both wild and mutated types of actin in order to study the changes in actin–myosin interactions under the effects of S350L.

Materials and methods

Sequence retrieval and analysis

The full amino acid length of adult human skeletal muscles myosin, myosin heavy chain 1 (MYH1: Accession: P12882.3, GI: 22669417), has been used with 1939 amino acids sequence length. In addition, actin query was obtained using human alpha-actin (Accession: AAB59376.1 GI: 178029) with 377 amino acids. This data have been taken from UniProt (http://www.uniprot.org/) and NCBI (http://www.ncbi.nlm.nih.gov/). PSI-BLAST and BLAST-PDB (http://blast.ncbi.nlm.nih.gov/Blast.cgiwas) were run for the analysis of the amino acid sequences.

Building and analyzing the 3D-models

Since human myosin crystallography has not been reported yet, the protein was modeled based on some non-human protein structures using EasyModeller 2.1. As the lever arm is unstable due to the lack of light chains, only head domain of the protein containing the

*Corresponding author. Email: shahir@fbb.utm.my

first 759 amino acids was modeled. It is understood that actins strongly interact with myosins during a power stroke, therefore, 1W8J has been chosen as a template that is in a strong binding form (Lorenz & Holmes, 2010). Actin has been modeled based on the top score PDBs of JPred which are different chains of 4WYB. Further, in the 3D structure of actin, Serine 350 was mutated to Leucine using PyMol.

The constructed models were then verified based on the highest value of template modeling (TM)-score which is calculated by the TM-align program. The TM-score is an important score for evaluating the quality of a model since it balances the root mean square deviation (RMSD) and the length of alignment. Therefore, TM-score is being broadly used in the assessment of 3D models. Online softwares such as PRO-CHECK, ERRAT, and VERIFY3D were used to evaluate the quality of models.

Molecular dynamic simulation

Molecular dynamic simulation has been used for various reasons such as analysis of effects of different ligands on protein's 3D structure (Kumar, Roopa, Mohammed, & Kulkarni, 2015), drug design (Kumar, Raj, Gupta, & Varadwaj, 2016), and investigation of the impacts of mutations on the structure and function of proteins (Palaniappan, Rao, & Ramalingam, 2016) through different software packages. In this study, energy minimizations of the constructed models were done using GROMACS 4.6.3 software package under OPLS-AA force field in suitably sized simulation cubic boxes. The sizes of cubic boxes for wild type of actin and S350L are 9.55 nm with 1 nm distance between protein and the cube while it is 12.87 nm with 1.25 nm of the thickness of the water layer for MYH1.Berendsen (weak coupling methods) and Parrinello–Rahman pressure coupling barostat (extended ensemble algorithm) were performed on both wild and mutated types of actin and MYH1 at normal body temperature (37 °C or 310 K) for 100 ns. Solvation of proteins was done using simple point charge (SPC) 216 water molecule under – genbox program. In order to include flexible water molecules rather than the rigid ones – DFLEXIBLE option was applied in em.mdp file. The system was then neutralized with Cl^- or Na^+. The gen-seed number (random generators for random velocities) that was used here is the default gen-seed number (173529). The final structure at the end of the molecular dynamics (MD) trajectories was chosen as the docking structures.

These structures are expected to demonstrate the best quality of proteins geometries and folding validities. To validate the fluctuations of residues in wild and mutated types of actin, simulations were run with two other gen-seed numbers. The number of atoms in myosin and actin (wild and muted types) before simulations and the number of water molecules, chlorine, and sodium ions used in the simulations are shown in Supplementary Table S1.

Hydrogen bond formation analysis

The hydrogen bonds between MYH1 and both wild and mutated types of actin in the position 350 were analyzed using the standard Autodock parameters. AutoDock reports the best docking solution (lowest docked free energy) for each GA run and also performs a cluster analysis in which the total number of clusters and the rank of each docking mode (cluster rank) were reported. Therefore, for a 100 GA run, there would be up to 100 total docking modes. Docking modes were selected based on two criteria: their proximity to the active site residues of myosin and extent of the interactions of actin with the interacting hydrophobic amino acid side chains of myosin. To achieve that the PDB file of myosin was docked with PDB files of both wild and mutated types of actin using AutoDock 4.2. Hydrogen atoms were added and merged to non-polar atoms in order to prepare the macromolecule and the ligand for docking. Furthermore, the Kollman charges computed by Gesteiger were added to the system. Then, Lysine 639 of MYH1and other amino acids of its loop (Glycine 637–Glycine 640) were set in a grid box. Two hydrogen bonds were formed between the oxygen atom of Lysine 639 and hydrogen atoms of Glycine 25 and alcoholic group of Serine 350 of actin. Moreover, a hydrogen bond was formed between Glycine 637 of MYH1 and Aspartic acid 26 of actin. Docking of myosin head domain with actin was done only through residues 25, 26, and 350 of wild type of actin and S350L. During this step, a genetic algorithm (GA) was chosen with 100 numbers of GA run and its output was saved as a DPF file using Lamarckin GA (4.2). To analyze the docking process, the output was reclustered using tolerances of 0.5 1.0 2.0 and the results were obtained under RMS tolerance of 1.000. Based on the clustering diagram, the best hydrogen bond is the one with the minimum energy value.

MD simulation of myosin–actin complex

The docked complexes of wild type and S350L were simulated using GROMACS software package 4.6.3 adopting the OPLS-AA force field parameters. The protein structures were solvated in a cubic box of 14.2 nm length with 1.5 nm of the thickness of water layers, using periodic boundary conditions and the SPC water molecule model. The topology files of residues 25, 26, and 350 of wild type of actin and S350L were generated using the PRODRG server in the form of DRG files. The total charges of the systems were neutralized by

adding one chlorine ion to each cubic box of the complexes. The systems were then equilibrated at human body temperature (310 K) for 100 ps. The trajectory snapshots were taken for structural analysis every picosecond. RMSD, root mean square fluctuation (RMSF), and H-bonds between the protein and ligand in the docked complexes during the simulation were analyzed through Gromacs utilities g_rmsd, g_rmsf and g_hbond, respectively. Supplementary Table S2 shows the number of atoms in myosin and DRG files and the number of water molecules used in the simulations.

Results and discussion

Construction and evaluation of 3D models

The head domain of MYH1 and actin were modeled using EasyModeller 2.1. The lever arm or the neck domain of MYH1 is extremely unstable in the absence of essential and regulatory light chains. Thus, only the head domain of this protein was modeled. Nevertheless, only the head domain of MYH1 is relevant to this study. EasyModeller 2.1 was run for several times and the models with the highest score were chosen. The modeling evaluation scores are summarized in Supplementary Table S3. In the final step, Serine 350 was mutated to Leucine in the actin 3D structure using PyMol.

G-actin is composed of two domains; the bigger domain and the smaller one. Each domain consists of two subdomains. The smaller domain includes subdomain I (residues 1–32/70–144/338–377) and subdomain II (residues 33–69) and the bigger domain is made up of subdomain III (residues 145–180/270–337) and subdomain IV (residues 181–269). The predicted secondary structure by Jpred is almost the same as the model.

The head domain of myosin consists of two actin binding sites; upper and lower sites. Both binding sites interact with G-actins via electrostatics interactions and hydrogen bonds; however, the upper actin binding site is only involved with AC3 while the lower actin binding site is in connection with both AC1 and AC3 (Lorenz & Holmes, 2010).

Molecular dynamic simulation of actin

Both wild and mutated types of actin models were simulated using GROMACS 4.6.3 software package of OPLS-AA force field under the same temperature and pressure. The template protein (4WYB) was also simulated for validation of the wild-type simulation. As it is shown in Figure 1, RMSD of two models are very similar. This illustrates that the wild and mutated types are both stable in human body's condition. The stabilized PDBs were taken from the last frame of the RMSD graphs (Supplementary Figure S1).

The RMSF was obtained based on the atoms fluctuations on alpha carbon positions of amino acids. As it is shown in Figure 2 the RMSFs of the template (4WYB) and the wild type are closely similar. This gives validation to our simulations. The main difference between the wild type and S350L is in the residues of 352–357 which are less fluctuated in the mutated type. Therefore, it is suggested that the mutated type must be more rigid in these positions in comparison with the wild type (Figure 1).

The results of RMSF plots were verified by simulation of wild type and S350L under two other gen-seed numbers (130 and 1700). The resulted fluctuations of residues in wild and mutated types are very similar to the fluctuations of default gen-seed number which proves that the RMSF plots are reliable (Supplementary Figure S2).

The secondary structures of wild type and S350L were analyzed by do_dssp program in the next step. This analysis demonstrates that the secondary structures of proteins become stabilized during 100 ns of MD simulations in both wild and mutated types. In addition, the secondary structure of wild type is mostly in the form of turn after residue 350 for a few amino acids while it has an α-helix structure for S350L (Supplementary Figure S3).

Finally the radius of gyration of wild type and S350L were compared with each other by g_gyrate program. Both plots became stabilized around 2.25 nm after 45 ns of simulations. This result indicates that the mutation does not affect the distribution of actin around an axis. Moreover, the structure of proteins is stabilized after 100 ns of simulation (Supplementary Figure S4).

Comparison of the 3D structure of wild and mutated types

The wild and mutated types were fitted together using PyMol software. The main difference between these two structures is in the amino acids ranged from 352 to 357. In the wild type, one big α-helix is formed from Serine 340 to Serine 350, which is followed by a coil in the position of Leucine 351 and one turn from Serine 352 to Methionine 357. In the mutated type, Leucine 351 forms a coil but it is followed by a small α-helix from Serine 352 to Methionine 357 (Figure 2).

This phenomenon can be caused by mutation of Serine 350 to Leucine which is a high helix-forming propensity amino acid. It seems that the high total force power of Leucine 350, Leucine 351 and Methionine 357 (which is another high helix-forming propensity amino acid) is the reason for these changes (Supplementary Figure S5). The position of Serine 352 to Methionine 357 has been vastly changed after mutation. In addition, the number of hydrogen bonds has been increased due to the formation of the coils of α-helix (Supplementary Figure S6).

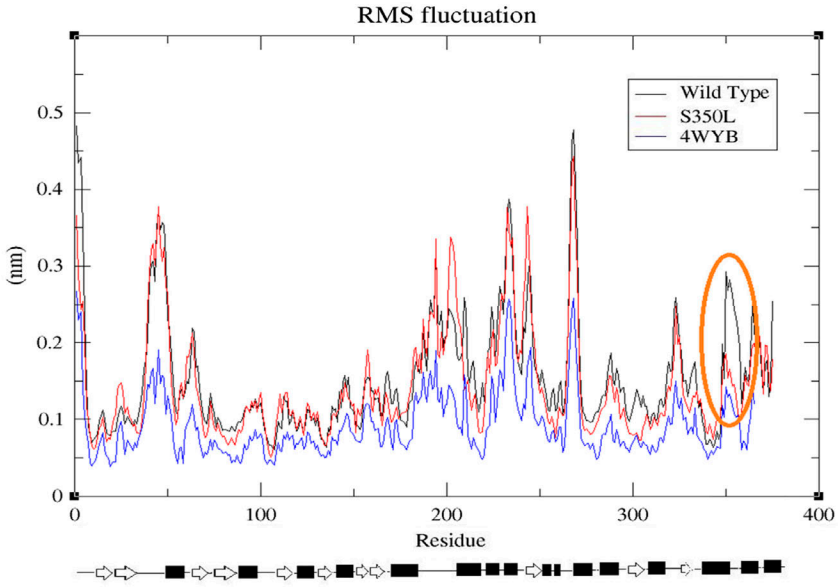

Figure 1. The RMSF comparison between the wild and mutated types of actin. The main difference can be observed at the mutation site where the mutated type shows less fluctuations. The design below the graph shows the secondary structure of wild type. The black squares are α-helixes and the flashes are β-sheets.

Figure 2. Superimposition of the wild and mutated types. The turn in the wild type and helix in the mutated type are colored in green and red, respectively.

After running the simulation, hydrogen bond and solvent accessible surface area (SASA) commands were applied from Serine 350 to Methionine 357 to compare the wild and mutated types in terms of the number of their hydrogen bonds and solvent accessibility. The results show that in average, the number of hydrogen bonds in S350L is two times more than the wild type at this segment which makes the mutated type more rigid. On the other hand, SASA has been decreased in mutated type since helixes are less solvent accessible comparing to loops. Furthermore, hydrophobicity in S350L has been increased mostly because of the formation of a helix but it can be also related to the replacement of Serine as a hydrophilic amino acid with Leucine as a hydrophobic residue (Supplementary Table S4).

Gelsolin is responsible for G-actin assembly and supports the structure of F-actin. In the wild type, hydrogen atom and alcoholic group of Serine 352 of actin form three H-bonds with oxygen atom and alcoholic group of Seine 428 of Gelsolin (Choe et al., 2002). After mutation, due to the formation of an α-helix, these groups were buried in the structure. Therefore, no H-bond is formed at this location (Figure 3). Consequently, the structure of F-actin becomes less stable and G-actins encounter a problem in their assembly.

Actin interacts weakly through Serine 352 to Lysine 361 with α-actinine (McGough, Way, & DeRosier, 1994) which is responsible for attaching F-actins to Z-lines of sarcomeres. In S350L, an α-helix has been formed from Serine 352 to Methionine 357, which seems that it prevents α-actinine from interacting with actin properly. This seems to be the main reason for F-actin aggregation in muscle fibers.

The aberrant helix is located on the outer layer of F-actin and it is exposed to water molecules. Both sides of F-actin have developed more hydrophobic surfaces than the wild type and these hydrophobic regions can bind through hydrophobic interactions. A decline in SASA and an increase in hydrophobicity in this part might be another reason for F-actin aggregation. F-actin aggregation disturbs the structure of sarcomere and causes the sliding speed of F-actin to drop.

Hydrogen bond formation analysis

Wild and mutated types were docked with the power stroke conformation of myosin's head domain. In the wild type, oxygen atom of Lysine 639 of myosin S1 forms two hydrogen bonds with Serine 350 alcoholic group of AC3 of F-actin and Glycine 25 NH group from its adjacent loop. Additionally, in the same loop of myosin S1, oxygen atom of Glycine 637 forms a hydrogen bond with Aspartic acid 26 NH group.

When the mutated type of actin was docked with myosin, the hydrogen bond between amino acid 350 of actin and Lysine 639 of myosin was lost. Since in this case an alcoholic amino acid has been replaced with a non-polar amino acid, the mutated amino acid is unable to form a hydrogen bond at the position of its R group (Figure 4). Therefore, the binding energy of myosin with S350L has increased to −3.57 comparing to the binding energy of wild type (−4.35). It seems that due to the aggregation of F-actins, myosin can hardly bind to actin monomers. If there is any binding between these two proteins, it will not occur at the position of residue 350. This fact can point out the severity of the disease.

Molecular dynamics simulation of myosin–actin complexes

The results of complex simulations for wild type and S350L show that both complexes were stabilized after 90 ns of simulation below 0.7 nm. Therefore, 100 ns of MD simulation is sufficient for energy minimizing of complexes (Supplementary Figure S7). The comparison of RMSF plots of wild and mutated complexes shows that the involved residues of myosin have similar fluctuations except at the position of residue 639. This residue is slightly more fluctuated in mutated complex comparing to the wild complex which is probably due to the lack of the H-bond with the residue 350 of actin (Supplementary Figure S8). The fluctuations of atoms in involved residues of actin, in myosin–actin interactions

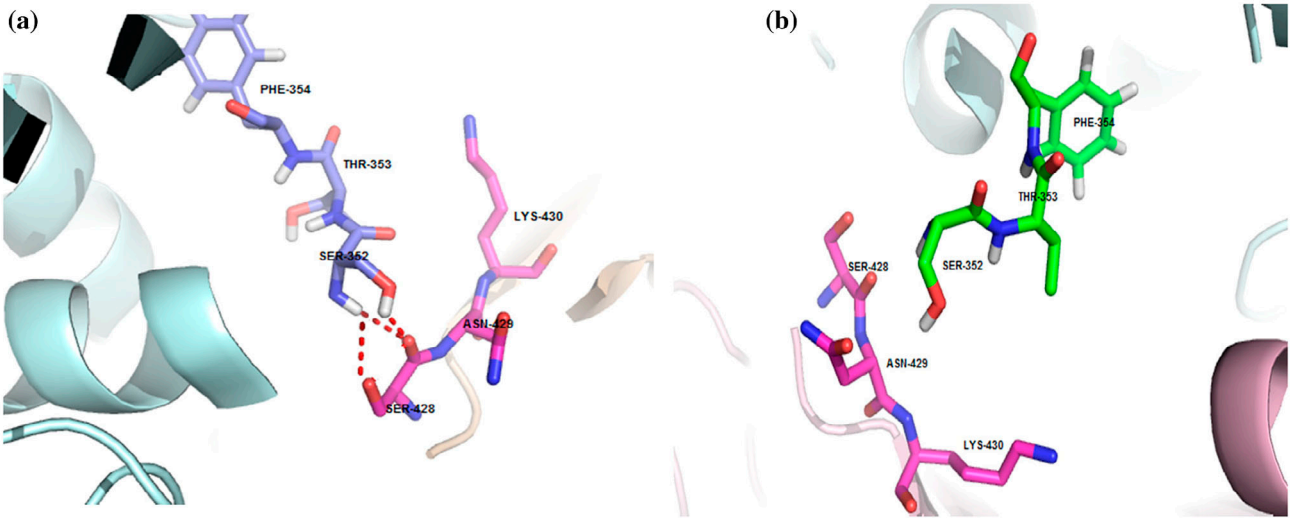

Figure 3. H-bond formation between actin and Gelsolin: (a) wild type and (b) S350L.

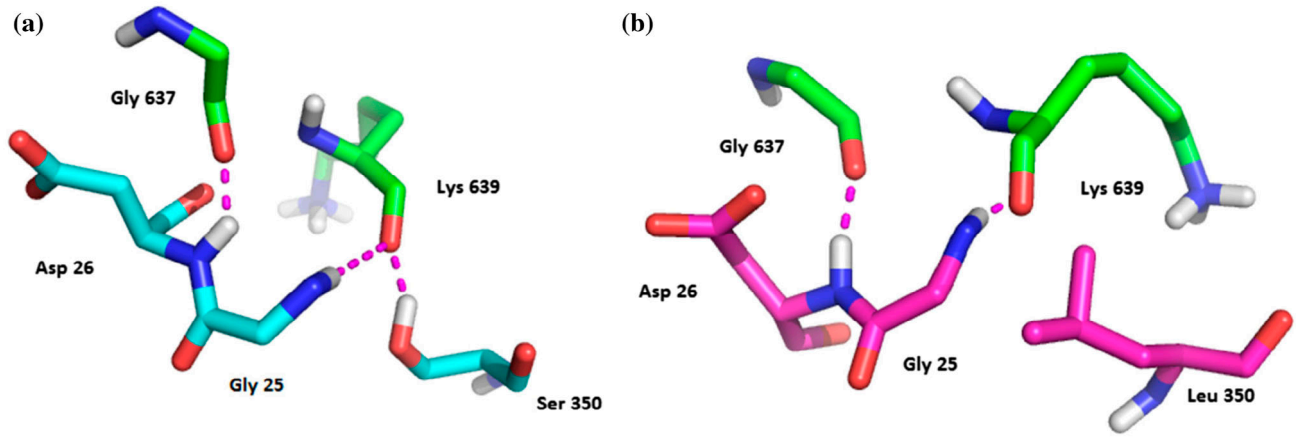

Figure 4. H-bond formation between myosin and actin in (a) wild type and (b) S350L. As it is illustrated in this figure, myosin does not form a H-bond with actin through Leucine 350 in the mutated type.

Table 1. The fluctuations of atoms of involved residues in wild type of actin in myosin and actin complex.

Glycine 25		Aspartic acid 26		Serine 350	
CAC	.0815	OD1	.1453	O	.1331
OAD	.0688	CG	.0405	C	.0715
CAB	.1052	OD2	.1047	CA	.0645
NAA	.151	CB	.0564	N	.1171
HKL	.152	CA	.0442	H3	.0853
HKM	.1474	C	.094	H4	.1341
HAA	.0364	O	.1191	H2	.117
		N	.0573	CB	.0967
		H2	.1112	OG	.1378
				HG	.0842

Table 2. The fluctuation of atoms of involved residues of S350L in myosin and S350L complex.

Glycine 25		Aspartic acid 26		Leucine 350	
CAC	.0789	OD1	.1237	O	.1587
OAD	.0626	CG	.0337	C	.1042
CAB	.1207	OD2	.1198	CA	.1283
NAA	.188	CB	.0509	N	.0951
HKL	.1891	CA	.0368	H3	.156
HKM	.1688	C	.1037	H4	.098
HAA	.0367	O	.1246	H2	.114
		N	.0557	CB	.1579
		H2	.1073	CG	.1747
				CD2	.183
				CD1	.2137

are shown in Tables 1 and 2. According to these tables, the atoms of Leucine 350 in mutated type are more fluctuated than in Serine 350 of wild type. The results of RMSD and RMSF show that both complexes are stabilized. Therefore, both wild and mutated types have formed stabilized H-bonds with myosin.

All trajectory frames were taken from the system from start to 100 ns in the PDB format. These PDBs were analyzed by VMD software in order to get the H-bond occupation frequencies of involved residues in myosin and actin interactions. In the wild complex, the H-bond occupancy between Glycine 25 of actin and Lysine 639 of myosin, Aspartic acid 26 of actin, and Glycine 637 of myosin and Serine 350 of actin and Lysine 639 of myosin are 63.45, 63.02, and 61.07%, respectively. Likewise, in the mutated complex these percentages are 62.17 and 61.13% for interactions between Glycine 25 of actin and Lysine 639 of myosin and Aspartic acid 26 of actin and Glycine 637 of myosin. Thus, all of H-bond occupancies in both wild and mutated complexes are around 60%. This indicates that the interaction between actin and myosin is not from a very strong nature and can be broken easily and separate them from each other after a muscle contraction. Furthermore, the H-bond occupancies show a reasonable stability for the hydrogen bonds formed in both complexes. Thus, wild type and S350L are stabilized during the interaction with myosin.

Conclusion

The results of this study give a solid reasoning for the accumulation of F-actins in the muscle fibers caused by a mutation in Serine 350. This mutation leads to the formation of an extra α-helix in actin from Serine 352 to Methionine 357. α-Actinine is a protein that binds weakly to Serine 352 and Lysine 359 and attaches F-actins to sarcomere. It seems that because of this mutated α-helix, α-actinine cannot attach to actin properly and

consequently, F-actins are not able to bind to Z-lines of skeletal muscle cells thoroughly. Moreover, SASA has been decreased and hydrophobicity has been increased in this segment on the surface of F-actin. Since this segment is exposed to a watery environment, the hydrophobic areas get closer to each other via hydrophobic interactions. The combination of these incidents results in the aggregation of F-actins in muscle fibers. On the other hand, wild actin interacts with Gelsolin through Serine 352. After the mutation, this interaction is lost which seems to make the structure of F-actin less stable. Generally, in the mutated complex myosin hardly interacts with actin due to the filament aggregations. Since this mutation occurs in the myosin–actin interaction interface, comparing the hydrogen bond formations in this location, shows that myosin does not interact with S350L in the location of Leucine 350. Despite all of that, myosin-S350L is a stable complex with stable hydrogen bonds. The results of this study can be used for further investigation on the effects of this mutation on the function of actin. Additionally, these findings may assist studies on other mutations in actin that causes actin filament aggregate myopathy.

Disclosure statement

No potential conflict of interest was reported by the authors.

Supplementary material

The supplementary material for this article is available online at http://dx.doi.org/10.1080/07391102.2016.1190299.

References

Choe, H., Burtnick, L. D., Mejillano, M., Yin, H. L., Robinson, R. C., & Choe, S. (2002). The calcium activation of gelsolin: Insights from the 3Å structure of the G4–G6/Actin complex. *Journal of Molecular Biology, 324*, 691–702. doi:10.1016/S0022-2836(02)01131-2

Dawson, J. F., Sablin, E. P., Spudich, J. A., & Fletterick, R. J. (2003). Structure of an F-actin trimer disrupted by gelsolin and implications for the mechanism of severing. *Journal of Biological Chemistry, 278*, 1229–1238. doi:10.1074/jbc.M209160200

Goebel, H. H., & Müller, H. D. (2006). Protein aggregate myopathies. *Seminars in Pediatric Neurology, 13*, 96–103. doi:10.1016/j.spen.2006.06.005

Kumar, H., Raj, U., Gupta, S., & Varadwaj, P. K. (2016). In-silico identification of inhibitors against mutated BCR-ABL protein of chronic myeloid leukemia: a virtual screening and molecular dynamics simulation study. *Journal of Biomolecular Structure & Dynamics, 1102*, 1–13. doi:10.1080/07391102.2015.1110046

Kumar, R. P., Roopa, L., Mohammed, M. M. S., & Kulkarni, N. (2015). Azadirachtin(A) distinctively modulates subdomain 2 of actin – Novel mechanism to induce depolymerization revealed by molecular dynamics study. *Journal of Biomolecular Structure and Dynamics, 1102*, 1–39. doi:10.1080/07391102.2015.1127665

Laing, N. G., Dye, D. E., Wallgren-Pettersson, C., Richard, G., Monnier, N., Lillis, S., … Nowak, K. J. (2009). Mutations and polymorphisms of the skeletal muscle α-actin gene (ACTA1). *Human Mutation, 30*, 1267–1277. doi:10.1002/humu.21059

Lorenz, M., & Holmes, K. C. (2010). The actin-myosin interface. *Proceedings of the National Academy of Sciences, 107*, 12529–12534. doi:10.1073/pnas.1003604107

McGough, A., Way, M., & DeRosier, D. (1994). Determination of the alpha actinin-binding site on actin filaments by cryoelectron microscopy and image analysis. *The Journal of Cell Biology, 126*, 433–443.doi:10.1083/jcb.126.2.433

Palaniappan, C., Rao, S., & Ramalingam, R. (2016). Unraveling the molecular effects of mutation L270P on Wiskkot–Aldrich syndrome protein: insights from molecular dynamics approach. *Journal of Biomolecular Structure and Dynamics, 1102*, 1–12. doi:10.1080/07391102.2015.1104263